

# Pattern, Growth and Aging in a Colony of Clustering Active Swimmers

Subir K. Das

*Theoretical Sciences Unit, Jawaharlal Nehru Centre for Advanced Scientific Research,  
Jakkur P.O., Bangalore 560064, India*

(Dated: July 31, 2021)

## Abstract

Via molecular dynamics simulations, we study the kinetics in a phase separating active matter model. Quantitative results for the isotropic bicontinuous pattern formation, its growth and aging, studied, respectively, via the two-point equal-time density-density correlation function, the average domain length and the two-time density autocorrelation function, are presented. Both the correlation functions exhibit basic scaling properties, implying self-similarity in the pattern dynamics, for which the average domain size exhibits a power-law growth in time. The equal-time correlation has a short distance behavior that provides reasonable agreement of the corresponding structure factor tail with the Porod law. The autocorrelation decay is a power-law in the average domain size. Apart from these basic similarities, the quantitative behavior of the above mentioned observables are found to be vastly different from those of the corresponding passive limit of the model which also undergoes phase separation. The functional forms of these have been quantified. An exceptionally rapid growth in the active system occurs due to fast coherent motion of the particles, mean-squared-displacements of which exhibit multiple scaling regimes, including a long time ballistic one.

## I. INTRODUCTION

Interest related to phase transitions [1] in active matters [2] stems from the fascinating clustering phenomena [2] in, e.g. a flock of birds, a colony of bacteria, etc. Typically, a steady state in active matter is the counterpart of the equilibrium in passive matter. Phase behaviors [3–6] of various active matter systems have been estimated experimentally and computationally. Critical exponents have been calculated for simple model systems [7–10]. Recently, the approach to the steady state, i.e., kinetics of phase transitions, has been a subject of immense interest [11–23].

Crucial questions in kinetics [24–29] relate to the type of pattern, its growth and aging, as a biological structure builds up from an embryo, of which, to our knowledge, aging has not been previously studied. Interfacial tension and transport mechanism control these in a passive system. Motility of the active particles is self-propelling [2], examples include microscopic bio-organisms to large animals. Even in a crowded environment this can be faster [30] than diffusion, typical single passive particle dynamics. Besides providing a faster collective dynamics, this can alter the interfacial tension. Thus, the kinetics in active matter is rather complex. Specific interest involves the scaling properties [25, 26], observed in passive matter, and the forms of various correlation and structure functions, alongside the domain growth law [25]. Here we address these issues, for isotropic percolating morphology in space dimension  $d = 3$ , via the molecular dynamics (MD) simulations [31, 32] of a phase separating model system, having both interparticle interactions and self-propelling activity. Existence of a phase transition in the passive limit of the model helps better quantitative understanding of the effects of activity.

Nature of a pattern can be understood from the two-point equal-time correlation function [25], which, in an isotropic case, is calculated as  $C(r, t) = \langle \psi(\vec{r}, t) \psi(\vec{0}, t) \rangle - \langle \psi(\vec{r}, t) \rangle \langle \psi(\vec{0}, t) \rangle$ ;  $r = |\vec{r}|$ . Here,  $\psi$  is a space ( $\vec{r}$ ) and time ( $t$ ) dependent order parameter. During the growth,  $C(r, t)$  obeys the scaling form [25]  $C(r, t) \equiv \hat{C}(r/\ell)$ , where  $\hat{C}$  is a master function and  $\ell$  is the average cluster size of a phase separating system. This scaling property reflects the self-similarity of the pattern during a typical power-law growth [25],  $\ell \sim t^\alpha$ . The exponent  $\alpha$  depends upon, among other factors, the transport mechanism [25]. For aging, besides other quantities, one studies the two-time order-parameter autocorrelation function [26]  $C_{\text{ag}}(t, t_w) = \langle \psi(\vec{r}, t) \psi(\vec{r}, t_w) \rangle - \langle \psi(\vec{r}, t) \rangle \langle \psi(\vec{r}, t_w) \rangle$ , where  $t_w$  ( $\leq t$ ) is the age of the system. While  $C_{\text{ag}}$  decays as a function of  $t - t_w$  in equilibrium (or in steady state), such time translation invariance does not hold when  $\ell$  has time dependence. During passive matter transitions,  $C_{\text{ag}}$  has the scaling form [26]  $C_{\text{ag}}(t, t_w) \equiv \hat{C}_{\text{ag}}(\ell/\ell_w)$ ,  $\ell_w$  being the length at  $t_w$ .

We observe that, in the active case also, both the correlations exhibit the scaling properties, implying self-similar growth. The structure factor,  $S(k, t)$ , Fourier transform of  $C(r, t)$ , closely follows the Porod law [33, 34]. Other than these, the structure and dynamics between the active and passive cases are vastly different. In the active case, even though the growth of  $\ell$  is algebraic, value of  $\alpha$  is very high, as in hydrodynamic growth, due to ballistic particle motion [6, 35] over long period, providing an advection-like collective transport. For  $r \gg 0$ , in the positive domain,  $C(r, t)$  decays as  $\exp(-r/\ell)$ , much slower than the passive case. The decay of  $C_{\text{ag}}$  is a power-law, differing qualitatively from passive hydrodynamics [36, 37]. Despite qualitative similarity of the decay with the Ising model kinetics [27], the exponent is different, which, nevertheless, obeys a lower bound [27].

## II. MODEL AND METHOD

In our model, two particles  $i$  and  $j$ , at distance  $r = |\vec{r}_i - \vec{r}_j|$  apart, interact via [38–40]  $u(r) = U(r) - U(r_c) - (r - r_c)(dU/dr)_{r=r_c}$ , where  $U(r) = 4\epsilon [(\sigma/r)^{12} - (\sigma/r)^6]$  is the standard Lennard-Jones (LJ) potential,  $\epsilon$ ,  $\sigma$  and  $r_c (= 2.5\sigma)$  being the interaction strength, particle diameter, and a cut-off distance (for faster computation), respectively. Phase behavior of this passive model in temperature ( $T$ ) - (number) density ( $\rho$ ) plane has been studied in  $d = 3$ . The critical temperature ( $T_c$ ) and density ( $\rho_c$ ) for the vapor-liquid transition [38] are approximately  $0.9\epsilon/k_B$  and  $0.3$ ,  $k_B$  being the Boltzmann constant.

We introduced the self-propelling activity via the Vicsek interaction [7, 8], where the direction of motion of a particle is influenced by the average direction ( $\vec{D}_N$ ) of its neighbors, contained inside the radius  $r_c$ . At each instant, every particle gets an acceleration  $f_A$  along  $\vec{D}_N$ . This, of course, will lift the temperature of the system, even in a canonical ensemble and is appropriate only for systems whose phase behavior is insensitive to temperature [5, 6]. To avoid this effect, in our temperature controlled transition, the amplitudes of the velocity vectors, after the kicks, were normalized to their values prior to the kicks, so that there is only a directional change. Other studies report that the Vicsek activity broadens the coexistence region [5, 6]. This was observed for this model as well. However, we will not present results on this aspect.

For this model, we have performed MD simulations [31, 32] with a Langevin thermostat, by solving the equation  $m\ddot{\vec{r}}_i = -\vec{\nabla}U_i - \gamma m\dot{\vec{r}}_i + \sqrt{6\gamma k_B T m} \vec{R}(t)$ , in periodic cubic boxes of linear dimension  $L\sigma$ , where  $m$  is the mass of a particle,  $U_i$  is the potential from interparticle passive

interactions,  $\gamma$  is a damping coefficient and  $\vec{R}$  is a noise having  $\delta$  correlation in space and time. A hydrodynamics preserving thermostat is avoided, since the objective is to see the effects of Vicsek activity. Presence of fast hydrodynamic mechanism may not allow us to identify the effects of activity. The Verlet velocity algorithm [31] was used with time step  $\Delta t = 0.01$ , in units of  $t_0 = \sqrt{\sigma^2 m / 48 \epsilon}$ . For the rest of the paper, we set  $m$ ,  $\epsilon$ ,  $\sigma$ ,  $k_B$  and  $\gamma$  to unity. We have prepared the initial configurations at  $T = 10$  with  $f_A = 0$  and kinetics was studied after quenching these to  $T = 0.5$  with  $\rho = 0.3$ , for  $f_A = 0$  (passive) and 1 (active).

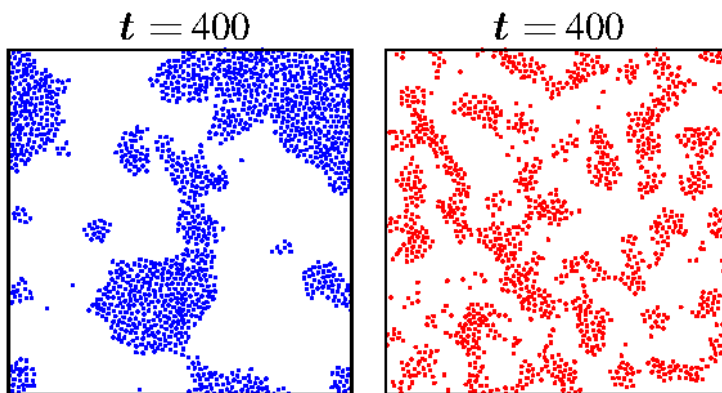


FIG. 1: 2D cross-sections of the snapshots at  $t = 400$  during the evolutions of the active (left frame) and passive (right frame) systems. In both the cases, the value of  $L$  is 64, for which the boxes contain  $N = 78644$  particles. For kinetics, all the passive model results were obtained for this particular system size whereas, the rest of the active matter results were obtained with  $L = 100$  ( $N = 300000$ ).

### III. RESULTS

In Figure 1 we present 2D cross-sections of snapshots during the evolutions of the active and the passive systems. Even though a lack of interconnectedness is seen, in 3D the morphologies are percolating. Given that the value of  $t$  is same in the two cases, it is clear that the coarsening in the active case is much faster. Another interesting noticeable difference is in the structure. A possible reason for this difference is that the Vicsek activity plays the primary role in the active matter structure formation, unlike the passive case where interfacial tension plays a crucial role [25]. To have a quantitative knowledge of the difference, we take a look at the  $C(r, t)$ .

In Figure 2 (a) we show the scaling plots of  $C(r, t)$  for the active system (symbols). For this calculation, we have mapped a continuum system onto a simple cubic lattice [38]. A lattice

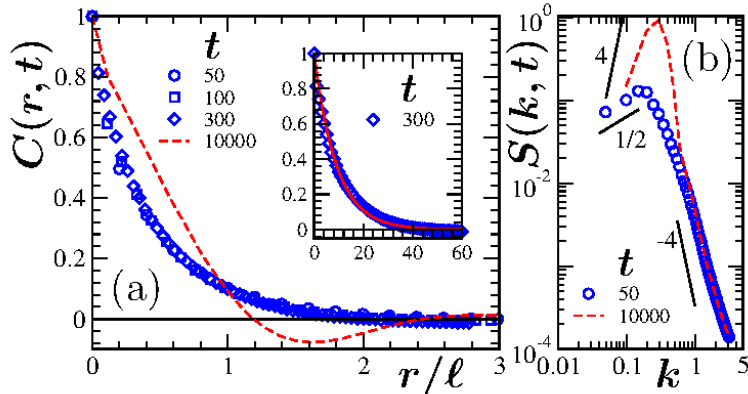


FIG. 2: (a) Plots of  $C(r, t)$  vs  $r/\ell$ , using data from different times. Symbols are for active system and the dashed line is for the passive system. Inset: Plot of  $C(r, t)$  vs  $r$  for the active system at  $t = 300$ . The solid line there is a fit to the form  $\exp(-r/\ell)$  for the data range  $[0, 40]$ . (b) Plots of  $S(k, t)$  as a function of  $k$  for the active (symbols) and passive (dashed line) systems. The solid lines are power-laws, the exponents for which are mentioned. The data sets are not normalized. The ordinates are appropriately scaled to superimpose large  $k$  data for the two cases. Here and for the following results the data were averaged over at least five independent initial configurations.

point was assigned an order-parameter value  $\psi = 1$  if the density (calculated using the nearest neighbor region) at that point is larger than  $\rho_c$ , otherwise  $-1$ . Nice collapse of data from different times confirms the self-similarity of the growing structure [25]. Thus, it is meaningful to extract the average cluster size from the decay of these functions and we obtained it from  $C(\ell, t) = 0.1$ .

The dashed line in Fig 2 (a) is the  $C(r, t)$  for the passive system. The difference between the two cases is overwhelming, the passive one having strong oscillations [41]. The absence of this aspect in the active case has similarity with the  $C(r, t)$  for the cluster growth during cooling in an assembly of inelastically colliding granular particles [41]. In the latter system, velocities of the particles become parallel after each collision. The Vicsek model produces similar parallelization effect and surface tension plays minimal role in deciding the structure. In that case, long distance behavior of the  $C(r, t)$  may have similarity with those for the single phase with large correlation length [42]. To be on the simpler side and keeping the small  $r$  singularity, related to Porod tail (a consequence of scattering from the interfaces), in mind, in the inset we use the form  $\exp(-r/\ell)$  to fit an unscaled active system  $C(r, t)$  in the range  $[0, 40]$ . At very large  $r$ ,  $C(r, t)$  will have negative values, before finally decaying to zero, due to the order parameter conservation constraint [43]  $\int C(r, t) d\vec{r} = S(0, t) = 0$ . Thus, while fitting to this form, it is mandatory to exclude data for

such extreme limit. The fit looks certainly good. In fact a good linear behavior can be seen on a log-linear plot, for  $C(r, t) > 0.05$ , up to  $r/\ell$  significantly larger than unity. This is a much slower decay than even the Ohta-Jasnow-Kawasaki function [25] for the nonconserved order-parameter dynamics and is expected to influence the aging property significantly. An Ornstein-Zernike [42] type form provides a better fit, with the power-law exponent being close to zero.

In Figure 2 (b) we show the structure factors for the active (symbols) and the passive (dashed line) systems. In the long wave-vector region there is nice agreement between the two cases and except for very large  $k$  (where the data suffer from noise due to non-zero temperature) the tails are reasonably consistent with a decay (albeit over a narrower range of  $k$  in the active case)  $\propto k^{-(d+1)}$ , the Porod law [33] in  $d = 3$ , for a scalar order parameter. The exponent  $\beta = 4$  corresponds to the Yeung's law [43], for small  $k$  power-law ( $k^\beta$ ) enhancement of  $S(k, t)$ . The value of  $\beta$  appears to be  $\simeq 1/2$  (which decreases with time) for the active dynamics, a consequence of slow decay of the  $C(r, t)$ , which will be further discussed in the context of aging. These results are at variance with the understanding that patterns are independent of the kinetic mechanism [44]. In the passive context, it was indeed demonstrated [45] that irrespective of a diffusive or a hydrodynamic growth,  $C(r, t)$  remains unchanged. This highlights the complexity of active matter phase separation.

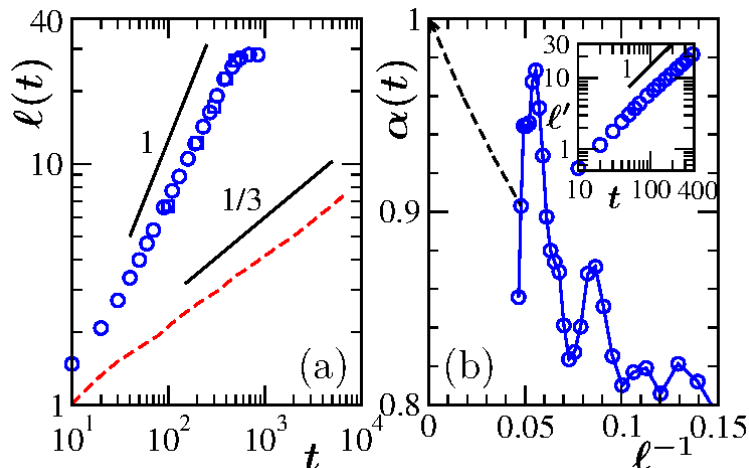


FIG. 3: (a) Plots of  $\ell$  vs  $t$ , for active (symbol) and passive (dashed line) systems. The solid lines correspond to different power-laws, exponents for which are mentioned. For the active case, the circles correspond to  $C(\ell, t) = 0.1$  and the squares (appropriately scaled to superimpose with the circles) are from exponential fits to the  $C(r, t)$ . (b) The time dependent growth exponent for the active system is plotted vs  $1/\ell$ . The dashed line is a guide to the eyes. The inset shows  $\ell'$  vs  $t$  (see text for details).

In Figure 3 (a) we present  $\ell$  vs  $t$  data, on a log-log scale. For both type of systems, power-laws are visible. The robustness of the exponential form for  $C(r, t)$  at all times, for the active case, can be appreciated from the fact that the values of  $\ell$  extracted from the corresponding fits (squares) are very much parallel to the ones obtained from  $C(\ell, t) = 0.1$  (circles). For the passive case, given that the Langevin thermostat is a stochastic one, diffusive growth is expected, with  $\alpha = 1/3$ , the Lifshitz-Slyozov exponent [46]. The self-propelling activity drastically enhances this value, previously observed in other situations [12, 22, 23], after a brief period with  $\alpha = 1/3$ , to about unity, a behavior expected for a viscous hydrodynamic growth [47]. In both the cases, the long time values of the exponents appear little weaker than the quoted numbers. This is due to the presence of a non-zero initial length [48]  $\ell_0$ . For more accurate estimate of  $\alpha$  for the active case, in Figure 3 (b) we have presented the instantaneous exponent [49]  $\alpha(t)$  ( $= d\ln\ell/d\ln t$ ), as a function of  $1/\ell$ . Clearly, the exponent is approaching a value  $\simeq 1$ , asymptotically. In the inset of this figure, we show the log-log plot for  $\ell'$  vs  $t$ , where  $\ell' = \ell - \ell_0$ ,  $\ell_0 = 0.93$ . For a significant range of the length this data set appear almost perfectly parallel to the  $\alpha = 1$  line. In the passive case, we avoid such exercise, since the Ising value of  $\alpha$  is expected, which has been estimated previously via other more sophisticated analyses [48]. Our active matter result, combined with 2D studies [12, 23], indicate that the dimensionality dependence may be weaker than hydrodynamic phase separation in passive matter.

Such a fast, hydrodynamic like growth is possible if the Vicsek activity can produce an advection-like effect in the collective transport. Given that coherency is inherent in the Vicsek model, fast particle motion can support that possibility. In Figure 4 we have presented a comparative picture for the time dependence of the single particle mean-squared-displacements (MSD). This figure is for  $T = 1.15$ , outside the coexistence region. The results are very different, despite the fact that the passive MSD was obtained via MD runs in a microcanonical ensemble that perfectly preserves hydrodynamics [31]. While a diffusive behavior for the passive case starts at  $t \simeq 30$ , in the active case this is delayed beyond  $t = 100$ . This effect will be more pronounced inside the miscibility gap. However, there one needs to track particles belonging to the clustered regions only, making it difficult to obtain data over an elongated period. Interestingly, compared to the usual scenario, there exist multiple scaling regimes [30] for the active matter MSD. Early time ballistic behavior crosses over to a super-diffusive regime at an intermediate time scale. Before moving to the final diffusive regime, a very robust ballistic behavior appears once more. The first two regimes are connected to the passive interparticle interaction, whereas the long

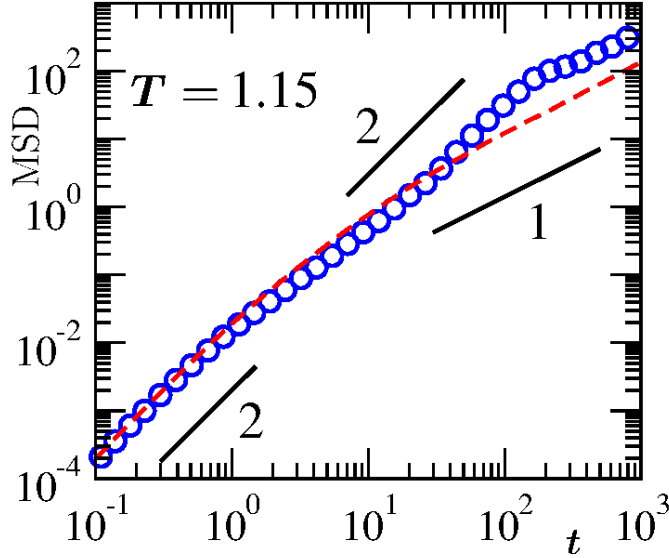


FIG. 4: Single particle MSDs are plotted vs time. The symbols are for the active case, whereas the dashed line is for the passive system. Unlike the other results, this figure corresponds to  $T = 1.15$  and  $L = 24$ . The solid lines are power-laws, exponents for which are mentioned.

time behavior is due to the Vicsek activity.

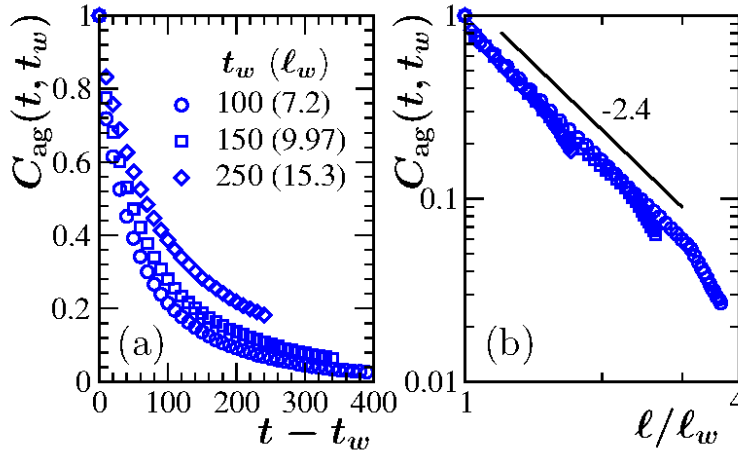


FIG. 5: (a) Plots of  $C_{ag}$  vs  $t - t_w$ , for the active case. Data for three different ages are presented. These values, along with the corresponding  $l_w$ , are mentioned. (b) Log-log plots of  $C_{ag}$ , vs  $l/l_w$ , for the same set of  $t_w$  values as in (a). The solid line is a power-law with exponent  $\lambda = 2.4$ .

Even though advection-like transport property in the active matter resembles hydrodynamic growth in fluids, these are not exactly the same, since the structure in the active case differs from



the universal passive form [44, 45]. Further differences may be observed in the aging property that we examine next. In Figure 5 (a), we show the plots of  $C_{\text{ag}}(t, t_w)$  vs  $t - t_w$ , for three different values of  $t_w$ , for the active case. As expected, no time translation invariance is obeyed. In Figure 5 (b) we plot  $C_{\text{ag}}(t, t_w)$  vs  $\ell/\ell_w$ . Nice collapse is seen, similar to the scaling property in passive transitions. Deviations from this, towards the tail of each data set, are due to the finite-size effects [50]. These are expected to appear at smaller values of  $\ell/\ell_w$  for larger  $t_w$ . On the log-log scale, the robust linear look implies a power-law decay [26],  $C_{\text{ag}}(t, t_w) \sim (\ell/\ell_w)^{-\lambda}$ . The data in the collapsed region provide  $\lambda = 2.4$ . This is remarkably different from the aging in hydrodynamic growth for which  $C(t, t_w)$  decays exponentially fast [36, 37]. Here note that, unlike the active case, no long range order in the velocity field was observed [45] even in (passive) hydrodynamic phase separation.

Prediction exists [26, 27] for a lower bound on  $\lambda$ , viz.,  $\lambda \geq (d + \beta)/2$ . Since  $\beta$  is significantly less than even unity, due to very slow decay of  $C(r, t)$ , the observed value, viz., 2.4, is consistent with this bound. This number, however, is even much smaller than the corresponding passive case [51] with diffusive kinetics, by accepting that the passive result will be same as the conserved Ising model. The difference in the values of  $\beta$  is partly responsible for this. The rest can be attributed to the fact that in the passive case domains can have fair degree of random motion, enhancing loss in memory. This effect should be more prominent in fluids, that leads to the exponential fall in  $C_{\text{ag}}(t, t_w)$ . On the other hand, even though fast hydrodynamic-like growth occurs due to coherent dynamics of the ballistically moving particles in active matter, such motion makes the movement of the domains more deterministic. In fact, it is reported [23] that the domains can slide along the interface, supporting our argument. Nevertheless, there exists scope for better understanding of this issue.

#### IV. SUMMARY

In conclusion, we have obtained a quantitative picture of the influence of self-propulsion on various aspects of kinetics of phase separation, viz., structure [25], growth [25] and aging [26], in a model of active matter, for bicontinuous morphology. The fundamental properties of phase ordering dynamics are obeyed, namely the scalings in the two-point equal-time and two-time autocorrelation functions are observed, implying a self-similar growth [25]. However, there exists significant quantitative difference between the active and passive matter kinetics.

A hydrodynamic like behavior [47] in the active matter domain growth is observed due to the fast coherent ballistic motion of the particles, leading to an effective advection in the collective dynamics. This, interestingly, makes the structure deviate from corresponding passive universal behavior. The correlation function shows nearly an exponential decay, much weaker than the passive case, except for small  $r$ . Consequently, the decay of the autocorrelation is also much slower than similar passive systems, though obeys a lower bound [43].

**Acknowledgment:** The author acknowledges comments from K. Binder and financial supports from Department of Science and Technology, Government of India; Marie-Curie Actions Plan of European Commission (FP7-PEOPLE-2013-IRSES Grant No. 612707, DIONICOS) and International Centre for Theoretical Physics, Italy.

- 
- [1] A. Onuki, *Phase Transition Dynamics* (Cambridge University Press, Cambridge, 2002).
  - [2] M.C. Marchetti, J.F. Joanny, S. Ramaswamy, T.B. Liverpool, J. Prost, M. Rao, and A. Simha, *Rev. Mod. Phys.* **85**, 1143 (2013).
  - [3] J. Schwarz-Linek, C. Valeriani, A. Cacciuto, M.E. Cates, D. Marenduzzo, A.N. Morozov, and W.C.K. Poon, *Proc. Natl. Acad. Sci. U.S.A.* **109**, 4052 (2012).
  - [4] J. Palacci, S. Sacanna, A.P. Steinberg, D.J. Pine, and P.M. Chaikin, *Science* **339**, 936 (2013).
  - [5] S.K. Das, S.A. Egorov, B. Trefz, P. Virnau, and K. Binder, *Phys. Rev. Lett.* **112**, 198301 (2014).
  - [6] B. Trefz, S.K. Das, S.A. Egorov, P. Virnau, and K. Binder, *J. Chem. Phys.* **144**, 144902 (2016).
  - [7] T. Vicsek, A. Czirók, E. Ben-Jacob, I. Cohen, and O. Shochet, *Phys. Rev. Lett.* **75**, 1226 (1995).
  - [8] A. Czirók and T. Vicsek, *Physica A* **281**, 17 (2000).
  - [9] G. Baglietto, E. V. Albano, and J. Candia, *Interface Focus* **2**, 708 (2012).
  - [10] H. Chaté, F. Ginelli, G. Grégoire, F. Peruani, and F. Raynaud, *Eur. Phys. J. B* **64**, 451 (2008).
  - [11] S. Mishra and S. Ramaswamy, *Phys. Rev. Lett.* **97**, 090602 (2006).
  - [12] J.M. Belmonte, G.L. Thomas, L.G. Brunnet, R.M.C. de Almeida, and H. Chaté, *Phys. Rev. Lett.* **100**, 248702 (2008).
  - [13] S. Mishra, A. Baskaran, and M.C. Marchetti, *Phys. Rev. E* **81**, 061916 (2010).
  - [14] M.E. Cates, D. Marenduzzo, I. Pagonabarraga, and J. Tailleur, *Proc. Natl. Acad. Sci. U.S.A.* **107**, 11715 (2010).
  - [15] G.S. Redner, M.F. Hagan, and A. Baskaran, *Phys. Rev. Lett.* **110**, 055701 (2013).

- [16] G.S. Redner, A. Baskaran, and M.F. Hagan, *Phys. Rev. E* **88**, 012305 (2013).
- [17] A. Wysocki, R.G. Winkler, and G. Gompper, *EPL* **105**, 48004 (2014).
- [18] E. Méhes, E. Mones, V. Németh, and T. Vicsek, *PLoS ONE* **7**, e31711 (2012).
- [19] S. Dey, D. Das, and R. Rajesh, *Phys. Rev. Lett.* **108**, 238001 (2012).
- [20] F. Peruani and M. Bär, *New. J. Phys.* **15**, 065009 (2013).
- [21] S. Mishra, S. Puri, and S. Ramaswamy, *Phil. Trans. R. Soc. A* **372**, 20130364 (2014).
- [22] P. Cremer and H. Löwen, *Phys. Rev. E* **89**, 022307 (2014).
- [23] E. Mones, A. Czirók, and T. Vicsek, *New. J. Phys.* **17**, 063013 (2015).
- [24] K. Binder, in *Phase Transformation of Materials*, Vol.5, p.405, edited by R.W. Cahn, P. Haasen, and E.J. Kramer (VCH, Weinheim, 1991).
- [25] A.J. Bray, *Adv. Phys.* **51**, 481 (2002).
- [26] D.S. Fisher and D.A. Huse, *Phys. Rev. B* **38**, 373 (1988).
- [27] C. Yeung, M. Rao, and R.C. Desai, *Phys. Rev. E* **53**, 3073 (1996).
- [28] G.F. Mazenko, *Phys. Rev. E* **69**, 016114 (2004).
- [29] F. Corberi, E. Lippiello, A. Mukherjee, S. Puri, and M. Zannetti, *Phys. Rev. E* **85**, 021141 (2012).
- [30] D. Loi, S. Mossa, and L.F. Cugliandolo, *Soft Matter* **7**, 10193 (2011).
- [31] D. Frenkel and B. Smit, *Understanding Molecular Simulations: From Algorithms to Applications* (Academic Press, San Diego, California, 2002).
- [32] M.P. Allen and D.J. Tildesley, *Computer Simulations of Liquids* (Clarendon, Oxford, 1987).
- [33] G. Porod, *Small-Angle X-Ray Scattering*, edited by O. Glatter and O. Kratky (Academic Press, New York, 1982).
- [34] Y. Oono and S. Puri, *Mod. Phys. Lett. B* **2**, 861 (1988).
- [35] Z. Wang, H.-Y. Chen, Y.-J. Sheng, and H.-K. Tsao, *Soft Matter* **10**, 3209 (2014).
- [36] S. Ahmad, F. Corberi, S.K. Das, E. Lippiello, S. Puri, and M. Zannetti, *Phys. Rev. E* **86**, 061129 (2012).
- [37] S. Majumder and S.K. Das, *Phys. Rev. Lett.* **111**, 055503 (2013).
- [38] S.K. Das, S. Roy, S. Majumder, and S. Ahmad, *EPL* **97**, 66006 (2012).
- [39] B.M. Mognetti, A. Šarić, S. Angioletti-Uberti, A. Cacciuto, C. Valeriani, and D. Frenkel, *Phys. Rev. Lett.* **111**, 245702 (2013).
- [40] V. Prymidis, H. Sielcken, and L. Fillion, *Soft Matter* **11**, 4158 (2015).
- [41] S.K. Das and S. Puri, *Phys. Rev. E* **68**, 011302 (2003).

- [42] M.E. Fisher, Rep. Prog. Phys. **30**, 615 (1967).
- [43] C. Yeung, Phys. Rev. Lett. **61**, 1135 (1988).
- [44] S. Puri, A. J. Bray, and J.L. Lebowitz, Phys. Rev. E **56**, 758 (1997).
- [45] S. Ahmad, S.K. Das, and S. Puri, Phys. Rev. E **85**, 031140 (2012).
- [46] I.M. Lifshitz and V.V. Slyozov, J. Phys. Chem. Solids **19**, 35 (1961).
- [47] E.D. Siggia, Phys. Rev. A **20**, 595 (1979).
- [48] S. Majumder and S.K. Das, Phys. Rev. E **81**, 050102 (2010).
- [49] D.A. Huse, Phys. Rev. B **34**, 7845 (1986).
- [50] J. Midya, S. Majumder, and S.K. Das, J. Phys.: Condens. Matt. **26**, 452202 (2014).
- [51] J. Midya, S. Majumder, and S.K. Das, Phys. Rev. E **92**, 022124 (2015).